Heliyon 10 (2024) e39533

Contents lists available at ScienceDirect

Heliyon

journal homepage: www.cell.com/heliyon

Research article

Transcriptomic analysis of embryonic mouse hypothalamic N38 cells exposed to high-energy protons and/or simulated microgravity

Nattha Suwanprakorn [a,b,1], Kyung-Ju Shin [a,b,1], Phuong Hoa Tran [a,b], Ngoc Thuan Truong [a,b], Kyu-Sung Kim [a,c], Hye Jin Yoo [b,d,*], Su-Geun Yang [a,b,**]

[a] Inha Institute of Aerospace Medicine, Inha University College of Medicine, Incheon, 22332, Republic of Korea
[b] Department of Biomedical Science, BK21 FOUR Program in Biomedical Science and Engineering, Inha University College of Medicine, Incheon, 22332, Republic of Korea
[c] Department of Otorhinolaryngology, Head and Neck Surgery, Inha University Hospital, Incheon, 22332, Republic of Korea
[d] Institute for Specialized Teaching and Research (INSTAR), Inha University, Incheon, 22332, Republic of Korea

ARTICLE INFO

Keywords:
Microgravity
Cosmic radiation
RNA sequencing
N38 embryonic mouse hypothalamus cell line
ZSCAN4 gene

ABSTRACT

Purpose: Space exploration poses unique challenges to astronauts, especially the effects of space radiation and microgravity (μG). Understanding molecular responses to these factors is crucial for ensuring astronaut health, and this study aimed to identify transcriptomic changes in mouse hypothalamic cell line N38 (mHypoE-N38) caused by simulated space environments.
Method: Four experimental groups were established, namely, a ground condition group (GC; the control group), a proton irradiated group (the space radiation group), a simulated μG group, and a proton irradiated × simulated μG group (the combination group). RNA sequencing and quantitative real-time polymerase chain reaction were performed to investigate key altered genes and to validate them.
Results: Three hundred and fifty-five differentially expressed genes were identified. Notably, the expressions of *UCN2* and *UGT1A5* genes were upregulated in all three experimental groups, suggesting a shared regulatory mechanism with potential consequences for brain function during space missions. Moreover, the study revealed significant alterations in genes belonging to the *USP17* and *ZSCAN4* families, indicating active response to DNA damage and telomere maintenance. PCR results validated that *UGT1A5*, *USP17* family, and *ZSCAN4* families (*ZSCAN4C*, *ZSCAN4D*, and *ZSCAN4F*) were significantly upregulated at the mRNA level in the combination group, while *UCN2*, *ZSCAN4A*, and *ZSCAN4B* were not reproduced.
Conclusion: The present study on mHypoE-N38 cells exposed to space environments revealed a complex molecular narrative with disease-oriented implications. The knowledge gained might serve as a cornerstone for developing strategies to mitigate potential health risks associated with extended exposure to space-related stressors.

* Corresponding author. Institute for Specialized Teaching and Research (INSTAR), Inha University, Incheon 22332, Republic of Korea. #501, Building B, 366 Seohae-daero, Jung-gu, Incheon, 22332, Republic of Korea.
** Corresponding author. Department of Biomedical Science, BK21 FOUR program in Biomedical Science and Engineering, Inha University College of Medicine, Incheon 22332, Republic of Korea #308, Building B, 366 Seohae-daero, Jung-gu, Incheon, 22332, Republic of Korea.
E-mail addresses: hyejin_yoo@inha.ac.kr (H.J. Yoo), Sugeun.Yang@inha.ac.kr (S.-G. Yang).
[1] The two authors contributed equally.

https://doi.org/10.1016/j.heliyon.2024.e39533
Received 26 July 2024; Received in revised form 10 October 2024; Accepted 16 October 2024
Available online 18 October 2024

1. Introduction

The challenges posed by space radiation and microgravity (μG) present formidable obstacles to human health and well-being during extended space travel [1,2]. Space radiation consists of high-energy particles emanating from the sun and cosmic sources that can penetrate spacecraft shielding and human tissue, and thus, poses risks of DNA damage and cellular mutation [3–5]. Moreover, μG alters physiological processes by removing the influence of Earth's gravity, and leads to changes in bone density, muscle mass, cardiovascular function, and other bodily systems [6,7]. These two stressors induce a cascade of biological responses at the genomic, epigenomic, and transcriptomic levels, triggering adaptive mechanisms to maintain homeostasis in the face of environmental perturbations [4]. Understanding the intricacies of these molecular adaptations is crucial for mitigating the health risks associated with space travel and ensuring the safety and well-being of astronauts during prolonged missions.

Genes lie at the core of molecular mechanisms, and the intricate interplay of genomic expressions underlies these mechanisms. Transcriptomics, comprehensive examinations of genetic expression changes, serves as a powerful tool for identifying potential alterations in molecular mechanisms. In the context of our study, transcriptomic analysis under simulated space conditions was utilized to explore mechanisms at the molecular level and enable a detailed examination of the effects of simulated space radiation and/or μG [8]. By scrutinizing transcriptomic changes, we aimed to gain insight into how these stressors impact gene expression patterns and elucidate resulting molecular responses induce by space-related challenges.

The present study was performed using embryonic mouse hypothalamic cell line N38 mHypoE-N38. This cell line was chosen because the hypothalamus is responsible for regulating the endocrine system, and thus, influences overall physiological processes, including hormone release, reproductive function, growth, fluid balance, and milk production [9]. Thus, understanding how the space environment, including μG and space radiation, affects the hypothalamus is crucial. Although this study was performed using a cell line, it provides a valuable approach for investigating the mechanisms whereby spaceflight stressors disrupt essential regulatory functions. Additionally, cell lines provide a controlled environment and enable cellular responses to μG and space radiation to be isolated and analyzed with greater precision than whole-animal studies. Finally, this focused approach enabled mechanisms possibly responsible for the disruption of the critical regulatory functions of the hypothalamus to be identified.

Our objective was to investigate genetic expressional changes induced by space radiation and/or μG using transcriptomic technology at the cellular level. Based on an understanding of how simulated space environments influence hypothalamic gene expressions, it is expected to provide noble insight into the potential health challenges faced by astronauts and contribute to the development of effective strategies that ensure their well-being during extended space endeavors.

2. Materials and methods

2.1. Cell culture and the study groups

mHypoE-N38 cells (Cedarlane Lab, Burlington, Canada) were seeded at a density of 1×10^5 cells in T25 flasks and cultured in Dulbecco Modified Eagle Medium (DMEM, high glucose; Gibco, Grand Island, NY, USA) supplemented with 10 % (*v/v*) heat-inactivated fetal bovine serum (FBS; HyClone, Logan, UT, USA) and 1 % (*v/v*) of penicillin-streptomycin (Gibco, Grand Island, NY, USA) in a humidified 5 % CO_2 atmosphere 37 °C. The medium was changed routinely every other day. Cells were divided into four groups: a ground condition group (GC; the control group), a proton irradiated group (the space radiation group), a simulated μG group, and a proton irradiated × simulated μG group (the combination group) (Fig. S1). For each group, cells were prepared in triplicate for each experiment (three T25 flasks per group for each experiment).

2.2. Exposure to simulated space radiation, μG, and combined conditions

Protons account for over 87 % of the radiation that astronauts are exposed to in space [10]. In the present study, T25 flasks (at a density of 1×10^5 cells) were irradiated with 1 Gy (Gy) of protons using a 100 MeV proton accelerator (TR102; Korea Multi-Purpose Accelerator Complex, Korea Atomic Energy Research Institute, Gyeongju-si, Republic of Korea). Since the effects of exposure were not immediately apparent, cells were subsequently cultured for 3 days, then cell pellets were obtained.

For μG simulation, a gravity controller, Gravite® (Space Bio-Laboratories Co., Ltd., Hiroshima, Japan), was used. This patented machine [patent no.: 623009 (JP) and US9494949B2 (US)] creates conditions similar to outer space (10^{-3} G) by rotating samples in 3D around two axes (inner and outer shaft), integrating the gravity vector with the temporal axis [11]. That is, μG is simulated at the center of the device when gravity vectors in a spherical space are added up. The machine offers preset rotation speeds with constant speed according to four modes (A to D). In this study, the recommended mode for cell culture (mode C) was used. Note that, real-time simulated μG values are displayed on the machine controller, allowing us to monitor the μG levels generated by the machine (Fig. S2). T25 flasks seeded with a cell density of 1×10^5 were securely fitted in the center of the machine, exposed to simulated μG for 3 days, and then cell pellets were collected.

To mimic the combined stress experienced by astronauts during spaceflight, we exposed mHypoE-N38 cells in T25 flasks (cell density 1×10^5) to a proton beam first, then, subjecting them to simulated μG for 3 days. This sequence enabled us to investigate how radiation damage and μG interact as the μG effect may diminish during post-irradiation incubation if μG exposure precedes radiation exposure. Same as other conditions, cell pellets were obtained after finishing the exposure to simulated space environment.

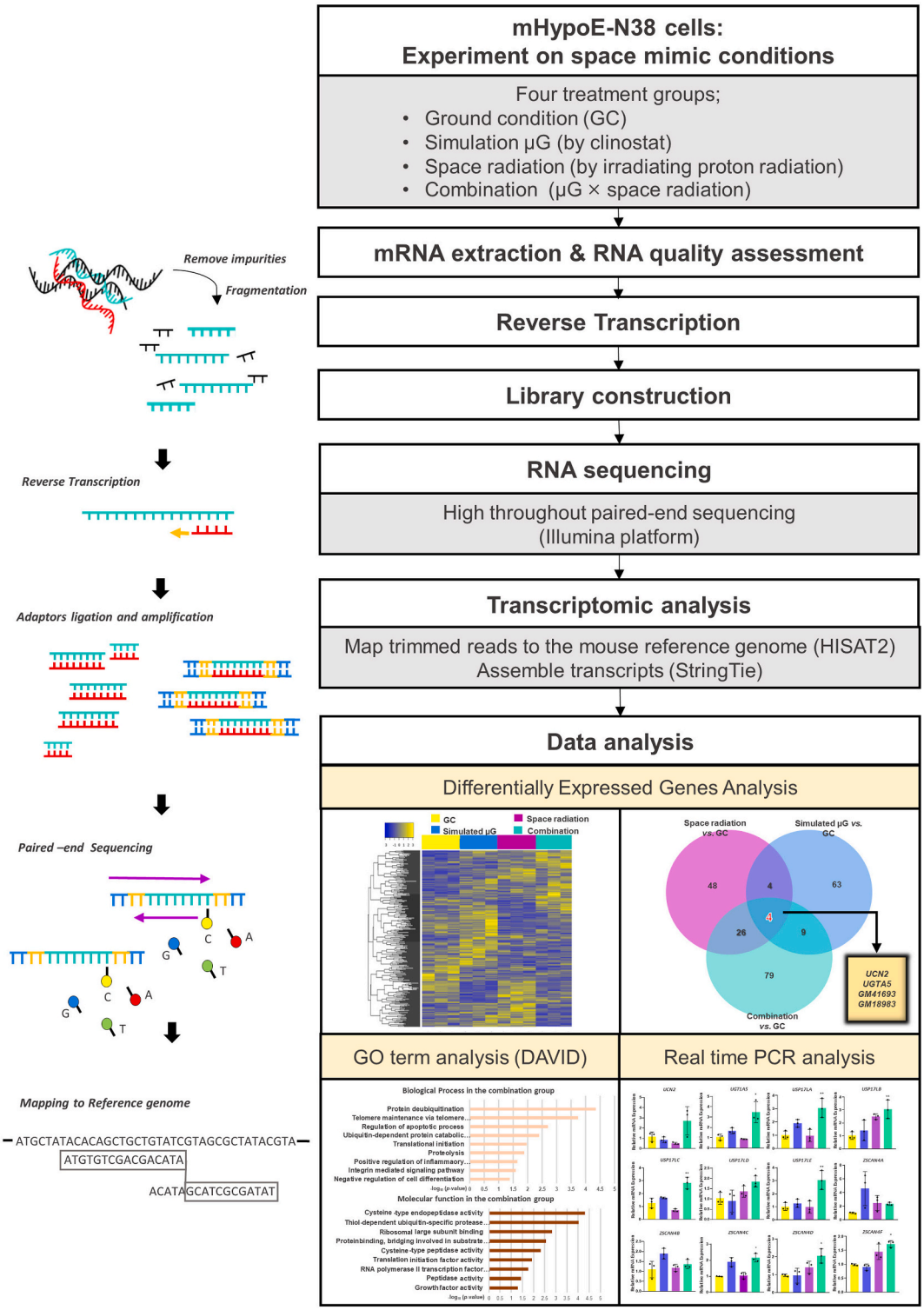

Fig. 1. Schematic of the experimental workflow.

2.3. RNA sequencing (RNA-seq)

A schematic of RNA sequencing (RNA-seq) workflow is provided in Fig. 1. Total RNA was extracted from cells in 25T flasks, and RNA integrity was confirmed using an Agilent 2100 Bioanalyzer (Agilent, Santa Clara, CA, USA). DNA contaminants were removed using DNase, and the RNA was then treated with a Ribo-Zero rRNA Removal Kit (Illumina, San Diego, CA, USA) to isolate the RNA for sequencing. Isolated and fragmented RNA were used to generate cDNA fragments by reverse transcription. For high-throughput sequencing, libraries were constructed using the TruSeq Stranded Total RNA Library Prep Kit with Ribo-Zero Human/Mouse/Rat (Illumina, San Diego, CA, USA). Library qualities and quantities were confirmed using the NovaSeq platform (Illumina, San Diego, CA, USA). Paired-end sequencing was performed using the Illumina platform (Illumina, San Diego, CA, USA), and sequencing reads were then mapped to the *Mus musculus* (mouse) reference genome (mm10) using HISAT2 software (http://www.ccb.jhu.edu/software/hisat). Transcript assembly was conducted using StringTie software (https://ccb.jhu.edu/software/stringtie), and expression values of transcriptomic profiles were obtained for each sample. The total number of reads generated by high-throughput sequencing and the percentage of those reads successfully mapped to the reference genome or transcriptome for each experimental condition are presented in Table S1. Mapping percentages ranged from 95.7 % to 97.4 %, indicating high overall data quality.

2.4. Quantitative real-time polymerase chain reaction (qRT-PCR)

To validate key gene expression changes, qRT-PCR was conducted. Given the high sequence similarities among some gene families, there is a possible risk of cross-mapping between genes, which could lead to over-counting during RNA-seq. To minimized this risk and ensure accurate validation of gene expression changes through qRT-PCR, the primer sequences for the target genes were designed and further validated using the NCBI website (https://www.ncbi.nlm.nih.gov/tools/primer-blast/). The specificity verification of the primers was then performed through melt curve analysis. By implementing these stringent primer design and validation steps, it was aimed to ensure that the primers: 1) bind uniquely to the desired target sequence within the gene family, and 2) avoid amplifying unintended sequences (cross-priming). The primer sequences are presented in Table S2. Total RNAs were extracted from mHypoE-N38 cells using Trizol reagent (Thermo Fisher, Waltham, MA, USA), and qRT-PCR was performed using a TB SensiFAST™ SYBR® Hi-ROX One-Step Kit (Meridian Bioscience Inc., Cincinnati, OH, USA) and a StepOne™ Real-Time PCR system (Thermo Fisher, Waltham, MA, USA). The PCR conditions used were 95 °C for 30 s followed by 40 cycles of 95 °C for 5 s, 60 °C for 30 s, and 72 °C for 30 s, followed by a final extension at 72 °C for 10 min. Melting curve analysis was performed at 95 °C for 15 s, 60 °C for 1 min, and 95 °C for 15 s. The relative mRNA expressions of differentially expressed genes (DEGs) were calculated using the $2^{-\Delta\Delta CT}$ method.

2.5. Western blot analysis for γ-H2AX detection

After performing RNA-seq and qRT-PCR experiment, the remaining sample were used to detect **γ**-H2AX (Fig. S1). Total proteins from the cell pellets were extracted using RIPA Lysis Buffer (Thermo Fisher, Waltham, MA, USA), with a protease inhibitor cocktail (GenDEPOT, Baker, TX, USA). The supernatant was collected after centrifugation at 13,000 g for 10 min at 4 °C. The total protein concentration was measured using a bicinchoninic acid (BCA) assay, with bovine serum albumin (BSA) (MP biomedicals, North Harbour, AUK, New Zealand) as the standard. The supernatant (protein sample) was then diluted with 5 × loading buffer and denatured at 95 °C for 10 min. Equal amounts of protein from each group (30 μg) and protein markers (iNtRON biotechnology, Seongnam-si, Republic of Korea) were separated using a 15 % SDS-PAGE gel. Proteins were then transferred to polyvinylidene fluoride (PVDF) membranes (Bio-rad, Hercules, CA, USA). After transfer, the membranes were blocked with Tris-buffered saline with Tween solution (TBST) (Biosesang, Seongnam-si, Republic of Korea) containing 5 % skimmed milk for 2 h at room temperature (RT). The membrane was then incubated overnight at 4 °C with primary antibodies against γ-H2AX (PA5-28778; Invitrogen, Waltham, MA, USA) and β-actin (AC004; ABclonal, Woburn, MA, USA), diluted in TBST containing 5 % BSA. The following day, the membranes were rinsed 3 times with TBST (10 min each) and again incubated with horseradish peroxidase (HRP)-conjugated secondary antibodies (7074S; Cell signaling technology, Danvers, MA, USA, and 7076P2; Cell signaling technology, Danvers, MA, USA), diluted in TBST containing 5 % skimmed milk for 2 h at RT. After completing the incubation, the membranes were rinsed three times with TBST (10 min each). Target proteins were detected using HRP substrate (Thermo Fisher, Waltham, MA, USA) and the signal were captured with blue sensitive X-ray film (Agfa, Septestraat, Mortsel, Belgium). Band quantification was performed using Image J (NIH, Bethesda, MD, USA).

2.6. Statistical analysis

RNA-seq data were analyzed using DESeq2, and differences between groups were identified using principal component analysis (PCA). *Pearson's* correlation coefficient analysis was performed to confirm the reproducibility of triplicate samples, and results were plotted as a heat map. Subsequently, volcano plot analysis was conducted to identify significant changes in gene expressions (DEGs) across groups using a |fold change| of ≥ 2 and a p-value of <0.05. Another heat map was created using *Pearson's* correlation coefficient analysis with hierarchical clustering to visualize intergroup correlations of DEGs. In addition, Database for Annotation, Visualization, and Integrated Discovery (DAVID; https://david.ncifcrf.gov), a web-based software package, was used to perform gene enrichment and functional analyses to understand biological processes and molecular functions associated with DEGs. Finally, qRT-PCR experiments were conducted, and the data obtained were analyzed using one-way ANOVA with Tukey's post-hoc test.

3. Results

3.1. Group similarity and data reproducibility

The PCA plot revealed distinct group-wise clustering (Fig. 2A), and thus, provided a visual representation of group similarities. *Pearson's* correlation coefficient analysis was conducted to confirm data reliability, and a heat map was generated (Fig. 2B). The high inter-sample similarity observed underscored the reproducibility of triplicate samples, thus strengthening the robustness of our dataset.

3.2. Global transcriptomic changes under simulated space conditions

RNA-seq data analysis revealed a comprehensive landscape of DEGs responses to the proton radiation, simulated μG, and combined treatment. Stringent criteria of a |fold change| ≥ 2 and a p-value of <0.05 were employed across the six pairwise group comparisons of the four study groups. Volcano plots of the six comparisons were generated to visualize significant differences in gene expressions across groups (Fig. 3A). As a result, 355 DEGs were identified. A heatmap of the 355 DEGs across the four study groups was generated to provide a visual representation of transcriptomic alterations (Fig. 3B). The distinct gene expression patterns observed underscored the influence of the three space-mimicked conditions. DEGs were classified by Venn-diagram analysis (Fig. 3C). Compared to the GC group, 82 were associated with simulated space radiation condition, 80 with simulated μG condition, and 118 with combined condition (Fig. 3C). Numbers of up- and down-regulated DEGs in the three experimental groups are shown in Fig. S3. This Venn-diagram analysis revealed four genes, *UCN2*, *UGT1A5*, *GM41693*, and *GM18983* were commonly affected, suggesting shared regulatory mechanisms (Fig. 3C). Among these genes, *GM41693* and *GM18983* are non-coding genes, while, intriguingly, *UCN2* and *UGT1A5* are associated with brain function. Therefore, *UCN2* and *UGT1A5* were viewed as key candidates for further investigation.

3.3. Functional annotation analysis and the key functional roles of the UPS17 and ZSCAN4 gene families

Since the effects of radiation and μG cannot be separated in space, we focused on comparing DEGs that were upregulated and downregulated in the combination and GC groups for the functional analysis. The comparison revealed that 76 genes were upregulated and 42 were down-regulated in the combination group (Fig. S3). Both up- and down-regulated DEGs were included in the analysis. The biological processes contributed to by DEGs were most significantly associated with protein deubiquitination ($p = 4.4 \times 10^{-5}$), with the *USP17* family being predominantly involved (Fig. 4A). This gene family is also related to the regulation of apoptosis ($p = 0.002$), ubiquitin-dependent protein catabolic processes ($p = 0.011$), and proteolysis ($p = 0.013$) (Fig. 4A). In addition, the second most DEG involvement was with telomere maintenance via telomere lengthening, particularly that associated with the *ZSCAN4* family (Fig. 4A). Interestingly, unlike *USP17*, *ZSCAN4* was exclusively associated with biological processes in the combination group (Fig. 4A and Fig. S4A), suggesting the combined treatment had a distinctive impact compared to the individual effects of space radiation or simulated μG.

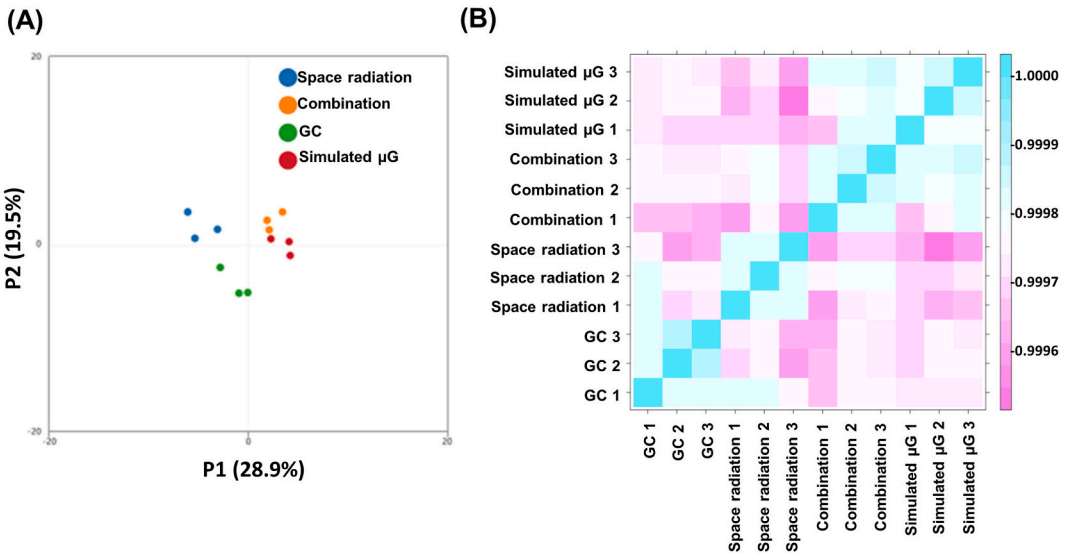

Fig. 2. Quality of RNA sequencing (RNA-seq) (A) PCA analysis. (B) Correlation matrix derived from *Pearson's* correlation coefficient [-1≤ *r* (correlation coefficient) ≤1] analysis. Blue indicates a positive correlation between samples, and pink indicates a negative correlation. An *r* value near 0 denotes a lack of linear association between variables (white). (For interpretation of the references to colour in this figure legend, the reader is referred to the Web version of this article.)

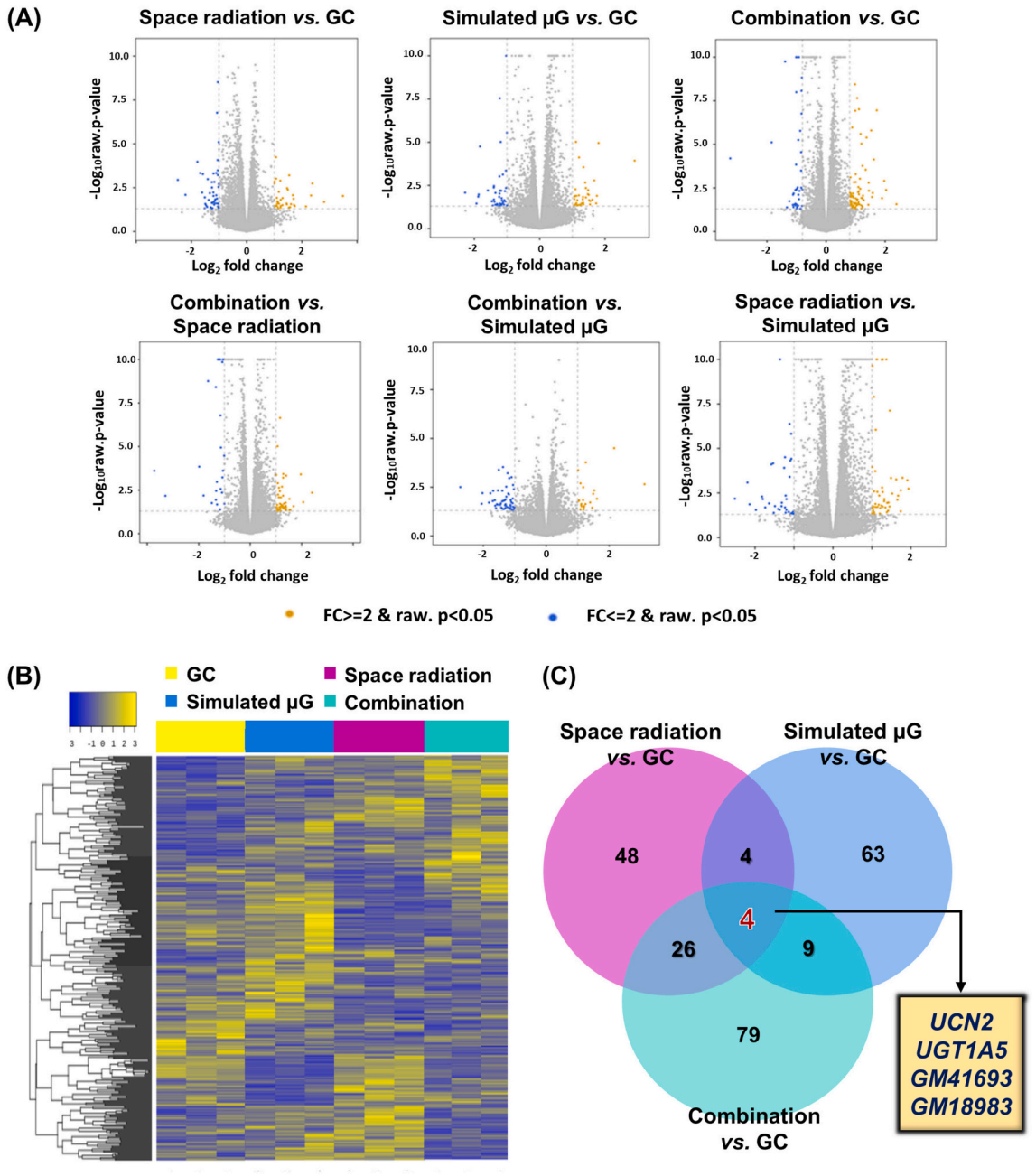

Fig. 3. Global transcriptomic changes under space-like conditions (A) Volcano plots displaying genes up- or down-regulated across group comparisons. (B) A heatmap of the 355 DEGs across groups. (C) Classification of the DEGs by Venn-diagram analysis.

In addition to biological processes, molecular function analysis revealed that the *USP17* family is notably involved in cysteine-type endopeptidase activity ($p = 4.8 \times 10^{-5}$) and thio-dependent ubiquitin-specific protease activity ($p = 9.5 \times 10^{-5}$) (Fig. 4B). In addition, *USP17* was related with other peptidase activities as well; cysteine-type peptidase activity ($p = 4.8 \times 10^{-3}$) and peptidase activity ($p =$ 0.036) (Fig. 4B). On the other hand, *ZSCAN4* was uniquely associated with RNA polymerase II transcription factor activity and sequence-specific DNA binding ($p = 0.017$) (Fig. 4B). These findings highlight the contribution of *USP17* to crucial cellular biological and molecular functions, and *ZSCAN4* that only appears particularly in the combination condition, as well. Other biological processes and molecular functions revealed by examinations of DEGs in the space radiation and simulated μG groups are provided in supplementary information (Fig. S4).

(A)

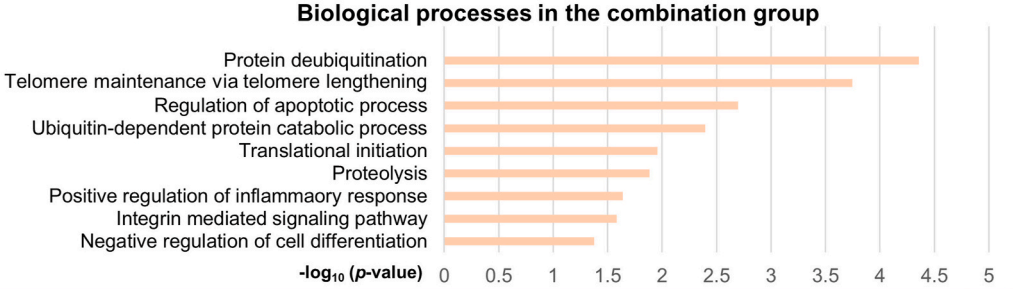

Biological Process	Identified genes	*p*-value	-log10 (*p*-value)
Protein deubiquitination	*USP17LA, USP17LB, USP17LC, USP17LD, USP17LE*	0.000044	4.36
Telomere maintenance via telomere lengthening	*ZSCAN4C, ZSCAN4D, ZSCAN4F*	0.00018	3.74
Regulation of apoptotic process	*USP17LA, USP17LB, USP17LC, USP17LD, USP17LE*	0.002	2.70
Ubiquitin-dependent protein catabolic process	*USP17LA, USP17LB, USP17LC, USP17LD, USP17LE*	0.004	2.40
Translational initiation	*EIF1AD2, EIF1AD6, EIF1AD8*	0.011	1.96
Proteolysis	*COLEC10, JMJD7, USP17LA, USP17LB, USP17LC, USP17LD*	0.013	1.89
Positive regulation of inflammatory response	*ITGA2,PDE2A,TSLP*	0.023	1.64
Integrin mediated signaling pathway	*FYB1,LIMS2, ITGA2*	0.026	1.59
Negative regulation of cell differentiation	*PRAMEL20, PRAMEL31, PRAMEL43*	0.042	1.38

(B)

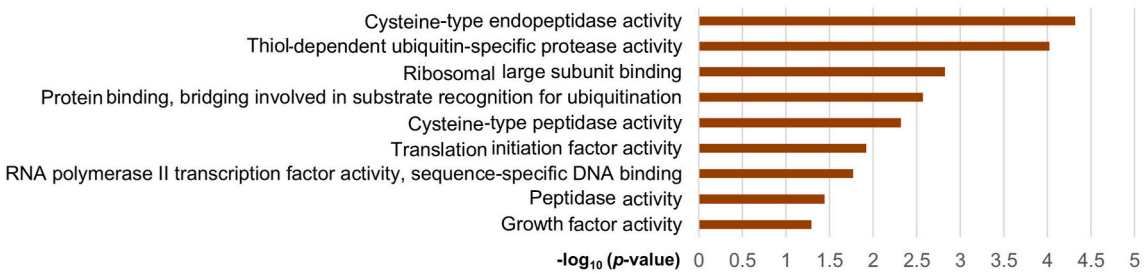

Molecular function	Identified genes	*p*-value	-log10 (*p*-value)
Cysteine-type endopeptidase activity	*USP17LA, USP17LB, USP17LC, USP17LD, USP17LE*	0.000048	4.32
Thiol-dependent ubiquitin-specific protease activity	*USP17LA, USP17LB, USP17LC, USP17LD, USP17LE*	0.000095	4.02
Ribosomal large subunit binding	*EIF1AD2, EIF1AD6, EIF1AD8*	0.0015	2.82
Protein binding, bridging involved in substrate recognition for ubiquitination	*PRAMEL20, PRAMEL31, PRAMEL39-PS, PRAMEL43*	0.0027	2.57
Cysteine-type peptidase activity	*USP17LA, USP17LB, USP17LC, USP17LD*	0.0048	2.32
Translation initiation factor activity	*EIF1AD2, EIF1AD6, EIF1AD8*	0.012	1.92
RNA polymerase II transcription factor activity, Sequence-specific DNA binding	*SP110, MZF1, ZSCAN18, ZSCAN4B, ZSCAN4B, ZSCAN4B, ZSCAN4B, ZFP352*	0.017	1.77
Peptidase activity	*JMJD7, USP17LA, USP17LB, USP17LC, USP17LD*	0.036	1.44
Growth factor activity	*CCN5, GDF15, NRTN*	0.051	1.29

Fig. 4. DAVID functional analysis of gene ontology (A) Biological processes and (B) Molecular functions were analyzed based on the 118 DEGs identified in the combination group.

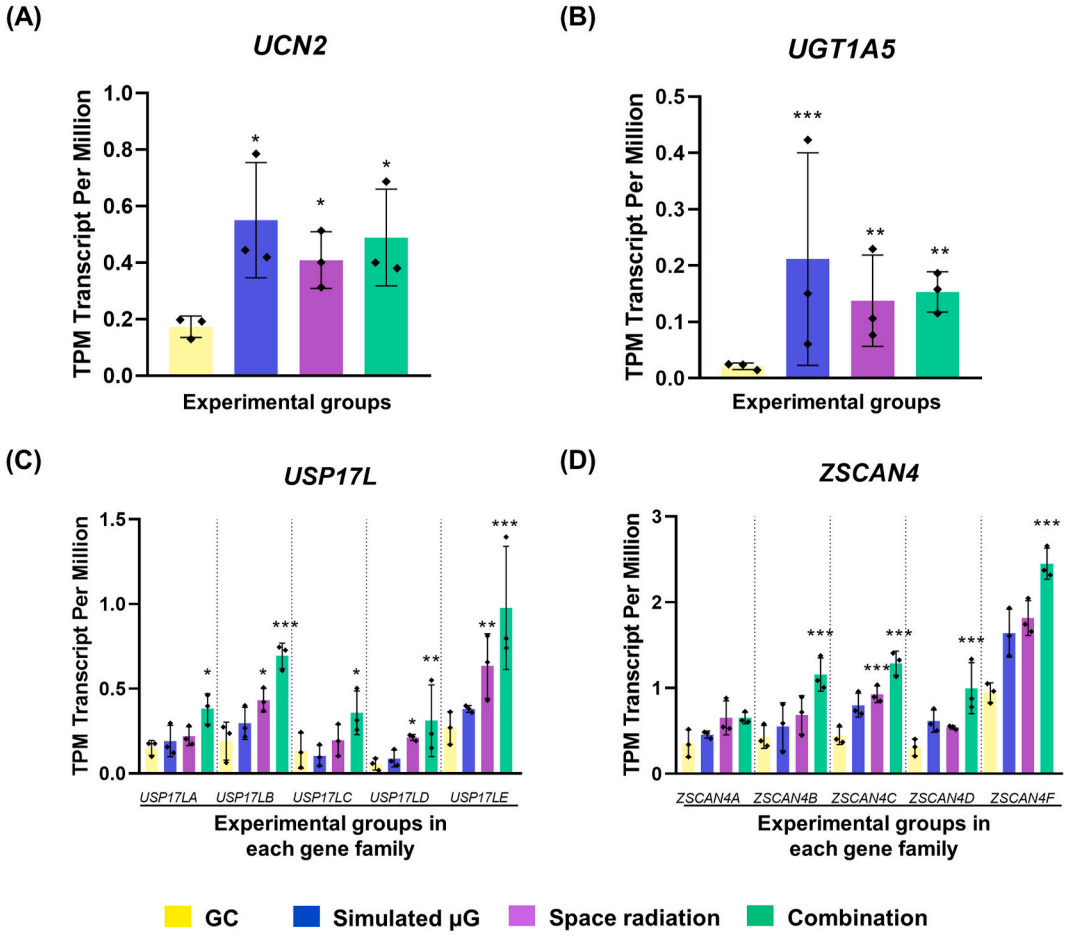

Fig. 5. Gene expressions of the key four genes, including *UCN2, UGT1A5, USP17 family*, and *ZSCAN4 family*, in the experimental groups
(A) The relative transcript number of *UCN2*. (B) The relative transcript number of *UGT1A5*. (C) The relative transcript number of the *USP17* family. (D) The relative transcript number of *ZSCAN4* family. *$p < 0.05$, **$p < 0.01$, and ***$p < 0.001$.

3.4. Genetic expression comparisons of the UCN2, UGT1A5, USP17 family and ZSCAN4 family in the study groups

The RNA expressions of *UCN2* and *UGT1A5* were significantly increased in the three experimental groups, especially in the simulated μG group (by 2.8- and 7.5-fold, respectively) (Fig. 5A and B). *UCN2* showed 2.2- and 2.4-fold increase in the space radiation and combination groups, respectively, and *UGT1A5* exhibited 5.19- and 5.5-fold increases in the space radiation and combination groups, respectively (Fig. 5A and B). For *USP17* family members (*USP17*LA, *USP17*LB, *USP17*LC, *USP17LD*, and *USP17*LE), upregulations were mostly observed in the simulated μG and space radiation groups, and especially, a significant increase was observed in the combination group (Fig. 5C). The expressions of *ZSCAN4* family members (*ZSCAN4A*, *ZSCAN4B*, *ZSCAN4C*, *ZSCAN4D*, and *ZSCAN4F*) were similarly influenced in the three experimental groups; however, *ZSCAN4A* did not show a significant upregulation in the combination group, unlike the other members (Fig. 5D).

3.5. Validation of key candidate DEGs and mRNA expressions

To validate RNA-seq data, qRT-PCR was performed on key candidate DEGs, including *UCN2*, *UGT1A5*, *USP17* family members, and *ZSCAN4* family members. The specificity of the primers for the genes of interest was validated using a melting curve with a single sharp peak (Fig. S5). While RNA-seq results demonstrated increased expressions of *UCN2* and *UGT1A5* under the simulated μG, space radiation, and combination groups, outcomes as determined by qRT-PCR analysis differed. Specifically, the combination group elicited a 2.41-fold increase in *UCN2* expression and a significant 3.5-fold increase in *UGT1A5* expression, whereas the simulated μG and space radiation groups failed to induce significant alterations (Fig. 6A and B). Regarding the *USP17* family, qRT-PCR revealed significant upregulations of *USP17*LA, *USP17*LB, *USP17*LC, *USP17LD*, and *USP17*LE genes specifically in the combination group (Fig. 6C–G), which concurred with RNA-seq results. Furthermore, a discernible trend was observed within the *ZSCAN4* family, showing significant 2.245-, 2.25-, and 1.79-fold increases in *ZSCAN4C*, *ZSCAN4D,* and *ZSCAN4F*, respectively, in the combination group. Unexpectedly,

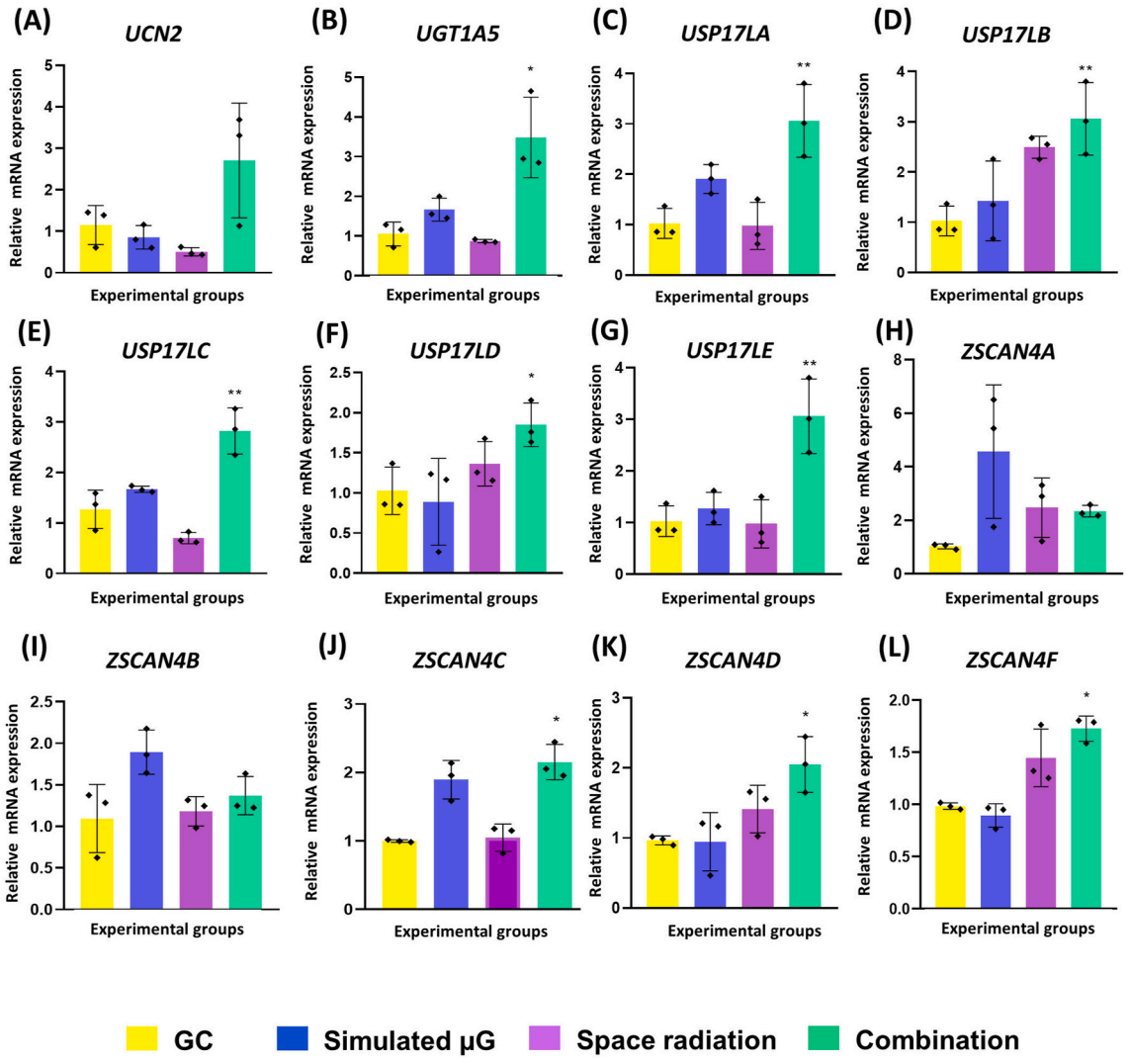

Fig. 6. Validation of the expression of *UCN2*, *UGT1A5*, *USP17* family, and *ZSCAN4* family under space-like conditions via qRT-PCR analysis The mRNA expression levels of (A) *UCN2*, (B) *UGT1A5*, (C–G) *USP17* family, and (H–L) *ZSCAN4* family under the ground condition (GC), simulated microgravity (μG), space radiation, and combination (μG × space radiation) conditions were validated in the independent experimental set.

the expressional change of *ZSCAN4B* in the combination group disappeared in the qRT-PCR analysis compared to the results of RNA-seq (Fig. 6H–L). Despite potential discrepancies that could have been attributed to batch variations, qRT-PCR results indicated that the combined effects of simulated μG and space radiation significantly amplified the differential expressions of the key DEGs, particularly in *UGT1A5*, *USP17* family members, *ZSCAN4C*, *ZSCAN4D*, and *ZSCAN4F*.

3.6. Degree of DNA damage under mimicked space environments

γ-H2AX is a well-known marker for DNA double-strand breaks (DSBs), which are induced by ionizing radiation such as space radiation. In the present study, the effects of proton irradiation at day 3 needed to be confirmed due to concerns about mitigating its effects compared to those observed immediately after irradiation (at day 1). Therefore, Western blot analysis for detecting γ-H2AX was additionally performed using the remaining samples. Unfortunately, the samples from the GC and simulated μG groups were not remained, and only one sample per remaining group left (Fig. S1). Consequently, the space radiation group at day 1 was set as a reference group, and statistical analysis could not be performed. Despite the limitations, as shown in Fig. S6, the protein expression of γ-H2AX in the space radiation group at day 3 exhibited a 1.65-fold increase. Although statistical significance could not be determined due to limited number of samples in each group, this result suggests that DNA damage worsens by day 3. Thus, the day-3 time point is deemed appropriate for assessing the effects of radiation. Meanwhile, the combination group at day 3 showed the highest γ-H2AX

levels, indicating synergistic effects of the combined conditions on DNA damage compared to the isolated space environment.

4. Discussion

This study identified 355 significant DEGs based on six group comparisons after exposing mHypoE-N38 cells to high-energy protons and/or simulated μG. Notably, each condition displayed distinct subsets of DEGs, underscoring the specificity of molecular responses to different stressors in outer space. In other words, the distinctions in DEGs between space radiation and simulated μG imply the complexity of biological responses in each space environment. In addition, the unique set of DEGs observed after combined treatment suggests an interaction effect not induced by individual stressors. In particular, two key coding DEGs, *UCN2* and *UGT1A5*, and two key functional gene families, *USP17* and *ZSCAN4*, were induced under the combination condition. Additionally, it is speculated that there are synergistic effects of the combined space condition as γ-H2AX, a marker for DSBs, exhibited the highest levels in the combination group compared to each individual space environment. This suggests that the increased expression of these genes in the combination group may reflect and associated with DNA damage under the given condition. Nevertheless, results involving *UCN2*, *ZSCAN4A* and *ZSCAN4B* should be carefully considered, as they were not fully reproduced in the PCR analysis.

UCN2 is a gene encoding urocortin-2, a member of corticotropin-releasing factor (CRF) family (CRF-peptides: CRF, UCN1, UCN2, and UCN3). This family plays a pivotal role in stress response mechanisms, with the activation of the hypothalamic-pituitary-adrenal (HPA) axis during stress being a fundamental function [12]. Thus, the induction of *UCN2* implies heightened sensitivity to stressors. Inflammation is a response to biological stress, and CRF-peptides have been reported to directly contribute to the modulation of the inflammatory response [13]. Tsatsanis C et al. revealed that CRF, UCN1, and UCN2 act as anti-inflammatory factors by suppressing tumor necrosis factor (TNF)-α at the early stage of the inflammation; whereas, they increase TNF-α production when the inflammation is prolonged, thereby inducing pro-inflammatory response. Similarly, Crucian BE et al. [14] reported that astronauts' plasma cytokines, including TNF-α, were elevated during long-duration spaceflight on the International Space Station (ISS). Additionally, a study claimed that UCN2 leads to macrophage apoptosis via a pro-apoptotic mechanism involving Bax and Bad proteins, ultimately suggesting an anti-inflammatory action of UCN2 [15]. Meanwhile, in behavioral aspects, an *in vivo* study demonstrated that UCN2 is related to anxiety and depression [16]. The study showed the potential of UCN2 as an anxiolytic and antidepressant drugs via its intracerebroventricularly treatment in mice [16]. During long-duration space missions, astronauts' anxiety and depression are significant risks that need to be addressed [17]. Therefore, this psychological function of UCN2 is noteworthy. Taken together, the increase in *UCN2* expression under the combined space environments may represent a natural biological countermeasure against inflammation, although the present study did not evaluate cytokine levels. Furthermore, careful consideration is needed to determine whether the elevation of *UCN2* expression can be utilized as an additional beneficial strategy for preventing anxiety and depression among astronauts.

UGT1A5 belongs to the *UGT1A* family and encodes a uridine diphosphate (UDP)-glucuronosyltransferase (UGT). Up to 22 UGT isoforms have been reported to be expressed in a tissue-specific manner in human [18]. In the brain, UGTs are mostly expressed in endothelial cells and astrocytes, which are the main components of the blood-brain barrier (BBB) [18]. They play a role in the detoxification barrier and modulation of endogenous compounds within the brain. In other words, the roles of UGTs in the BBB, where they participate in the transformation and elimination of various substances, are noteworthy. The regulation of compounds at the BBB is crucial for maintaining homeostasis within the central nervous system. However, BBB dysfunctions occur during spaceflight due to μG-induced fluid shifts toward the head and the susceptibility of the vasculature to radiation [19]. Thus, the induction of *UGT1A5* in response to the space environment suggests a potential adaptive response aimed at preserving the integrity of the internal environment of the brain in the presence of these unique stressors [18]. Note that, to the best of our knowledge, the present study is the first report of the *in vitro* expression of *UGT1A5* isoform in a hypothalamic cell line using RNA-seq and qRT-PCR. Moreover, *UGT1A4*, *UGT1A6*, and *UGT2B7* expression have been reported in the human brain [20], whereas expression of *UGT1A5* in this region has not been documented. Although the presence of UGT isoforms in the brain may vary between species, the basic function of UGTs responsible for the glucuronidation to increase the hydrophilic properties of diverse substances remains consistent. Therefore, further studies on the interaction between human brain UGTs and exposure to space radiation and μG are warranted in the field of space science.

It is well-known that radiation in space, which primarily consist of heavy ions from galactic cosmic rays (GCRs) and solar cosmic radiation (SCR), has high energy [21]. GCRs and SCR are ionizing radiation [21,22] that cause DNA damage, especially DSBs [23–26]. In the body, the DNA repair system is activated in the presence of DNA damage, and USP17 contributes to DNA repair by regulating the deubiquitination of the key DNA repair molecule, defective chorion-1 (DEC-1) [27]. In the present study, the 100 MeV proton beam was used for 1 Gy irradiation, which had enough energy to cause genomic damage [26]. Consequently, the upregulation of *USP17* family members observed in the space radiation group (Fig. 5C) might be a complementary reaction of DNA damage. Notably, both RNA-seq and qRT-PCR data consistently showed that the expression of *USP17* family members was much higher in the combination group compared to the other groups (Fig. 5C, 6C-6G), possibly indicating that μG had a synergistic effect on *USP17* expression. In addition, USP17 is known to have both oncogenic and tumor-suppressive effects by controlling various molecular pathways [27–30]. Given the known carcinogenic risks associated with space exploration [31], our findings also suggest a link between *USP17* and cancer risk.

ZSCAN4 is a well-established protein with a pivotal role in maintaining telomeres, which are essential for genomic stability as they protect chromosomes from being recognized as damaged DNA and inappropriate DNA damage responses [32–34]. Luxton et al. [35] revealed that telomere lengths were longer during spaceflights but shortened after spaceflight compared to their lengths before spaceflight. This suggests that telomere maintenance mechanisms are modulated by space environments, which agrees with our study observation of increased *ZSCAN4* expression in the combination group. In addition to telomere preservation, *ZSCAN4* also promotes

DNA repair by regulating poly (ADP-ribose) polymerase 1 (PARP1), a key member of the alternative non-homologous end joining (alt-NHEJ) pathway and primarily implicated in DSB repair system [36,37]. Indeed, in the combination group, *ZSACN4C*, *ZSCAN4D*, and *ZSCAN4F* exhibited significant increase in both RNA-seq and qRT-PCR analyses. As the combination group showed the highest levels of γ-H2AX (Fig. S6), indicating the induction of DSBs, the increase in these gene members may reflect a compensatory response to the DNA damage induced by the combined space environment. Meanwhile, the *ZSCAN4* family has been shown to be highly transiently expressed, particularly at the 2-cell stage and in mouse embryonic stem cells (mESC), with predominant expression of *ZSCAN4C* and *ZSCAN4D* [38]. Despite this transient expression, the three *ZSCAN4* members–*ZSCAN4C*, *ZSCAN4D*, *ZSCAN4F*–showed significantly increased expression in the E15∼17 mouse embryo, from which the cell line used in this study was derived, under the combined space condition. This may suggest a response to DNA damage. Finally, given the low expression of *ZSCAN4B* [38], the loss of significance of it in the combination group may be unlikely to impact the overall function of the *ZSCAN4* family. Although the expression result of all *ZSCAN4* members in RNA-seq were not perfectly replicated in qRT-PCR, our findings partially validated the increased expression of *ZSCAN4* in the combination group and supported the changes observed alongside the γ-H2AX result.

5. Conclusion

Our investigation into the single and combined impacts of high-energy protons and simulated μG on the mHypoE-N38 cell line unraveled a complex molecular narrative with potential disease-oriented implications. Particularly under the combined conditions, all DEGs except for *UCN2*, *ZSCAN4A*, and *ZSCAN4B* increased expression, suggesting a synergistic effect of space radiation and μG on transcriptomic changes. Notably, increased DSBs were also observed in the combination group; however, this finding requires re-validation due to the limited sample size and the lack of statistical analysis between the groups in this study. Nonetheless, the insight gained from this research may serve as a cornerstone for developing strategies aimed at mitigating the potential health risks associated with prolonged exposure to space-related stressors.

CRediT authorship contribution statement

Nattha Suwanprakorn: Writing – review & editing, Writing – original draft, Validation, Methodology, Investigation, Formal analysis, Data curation. **Kyung-Ju Shin:** Writing – original draft, Methodology, Investigation, Data curation, Conceptualization. **Phuong Hoa Tran:** Investigation. **Ngoc Thuan Truong:** Investigation. **Kyu-Sung Kim:** Conceptualization. **Hye Jin Yoo:** Writing – review & editing, Supervision, Formal analysis, Data curation. **Su-Geun Yang:** Supervision, Project administration, Methodology, Formal analysis, Conceptualization.

Key points

- During missions, astronauts are exposed to harsh environments such as various types of radiation and huge gravity differences, which are primary stressors in space.
- The hypothalamus serves as the central regulator of physiological functions and thus is a focus of research associated with space environments.
- This is the first transcriptomic study on the effects of proton radiation and/or simulated microgravity on mHypoE-N38 cells (a hypothalamus cell line).
- The expressions of the *UCN2*, *UGT1A5*, *USP17,* and *ZSCAN4* genes were altered by exposure to simulated space environments (RNA-seq).
- These expressional changes suggest potential loss of functions related to genomic instability and stress response following exposure to space environments.

Data availability

The raw data used in the present study is available at the NCBI repository via the following link: https://www.ncbi.nlm.nih.gov/sra/PRJNA1097775.

Funding

This work was supported by the Basic Science Research Program and the Korea Health Technology R&D Project through the National Research Foundation of Korea (NRF) and the Korea Health Industry Development Institute (KHIDI) funded by the Korean government (MOE, MOHW, and MSIT) [grant numbers: RS-2023-00208587, 2018R1A6A1A03025523, and RS-2023-00266209].

Declaration of competing interest

The authors declare that they have no known competing financial interests or personal relationships that could have appeared to influence the work reported in this paper.

Acknowledgment

The authors express their gratitude for the support provided by the Korea Multi-Purpose Accelerator Complex (Korea Atomic Energy Research Institute).

Appendix A. Supplementary data

Supplementary data to this article can be found online at https://doi.org/10.1016/j.heliyon.2024.e39533.

References

[1] E. Afshinnekoo, R.T. Scott, M.J. MacKay, E. Pariset, E. Cekanaviciute, R. Barker, et al., Fundamental biological features of spaceflight: advancing the field to enable deep-space exploration, Cell 183 (5) (2020) 1162–1184.
[2] F.E. Garrett-Bakelman, M. Darshi, S.J. Green, R.C. Gur, L. Lin, B.R. Macias, et al., The NASA Twins Study: a multidimensional analysis of a year-long human spaceflight, Science. 364 (6436) (2019).
[3] G.C. Demontis, M.M. Germani, E.G. Caiani, I. Barravecchia, C. Passino, D. Angeloni, Human pathophysiological adaptations to the space environment, Front. Physiol. 8 (2017) 547.
[4] M. Moreno-Villanueva, M. Wong, T. Lu, Y. Zhang, H. Wu, Interplay of space radiation and microgravity in DNA damage and DNA damage response, npj Microgravity 3 (1) (2017) 14.
[5] S. Wakayama, D. Ito, Y. Kamada, T. Shimazu, T. Suzuki, A. Nagamatsu, et al., Evaluating the long-term effect of space radiation on the reproductive normality of mammalian sperm preserved on the International Space Station, Sci. Adv. 7 (24) (2021).
[6] H.P. Nguyen, S. Shin, K.J. Shin, P.H. Tran, H. Park, Q. De Tran, et al., Protective effect of TPP-Niacin on microgravity-induced oxidative stress and mitochondrial dysfunction of retinal epithelial cells, Biochim. Biophys. Acta Mol. Cell Res. 1870 (1) (2023) 119384.
[7] J.W. Wolfe, J.D. Rummel, Long-term effects of microgravity and possible countermeasures, Adv. Space Res. 12 (1) (1992) 281–284.
[8] S. Ray, S. Gebre, H. Fogle, D.C. Berrios, P.B. Tran, J.M. Galazka, et al., GeneLab: omics database for spaceflight experiments, Bioinformatics 35 (10) (2019) 1753–1759.
[9] Z. Shahid, E. Asuka, G. Singh, Physiology, Hypothalamus. StatPearls. Treasure Island (FL): StatPearls Publishing Copyright © 2024, StatPearls Publishing LLC., 2024.
[10] K. Kumar, S. Kumar, K. Datta, A.J. Fornace, S. Suman, High-LET-radiation-induced persistent DNA damage response signaling and gastrointestinal cancer development, Curr. Oncol. 30 (6) (2023) 5497–5514.
[11] T. Furukawa, K. Tanimoto, T. Fukazawa, T. Imura, Y. Kawahara, L. Yuge, Simulated microgravity attenuates myogenic differentiation via epigenetic regulations, NPJ Microgravity 4 (2018) 11.
[12] M. Schäfer, S.A. Mousa, C. Stein, Corticotropin-releasing factor in antinociception and inflammation, Eur. J. Pharmacol. 323 (1) (1997) 1–10.
[13] C. Tsatsanis, A. Androulidaki, E. Dermitzaki, A. Gravanis, A.N. Margioris, Corticotropin releasing factor receptor 1 (CRF1) and CRF2 agonists exert an anti-inflammatory effect during the early phase of inflammation suppressing LPS-induced TNF-alpha release from macrophages via induction of COX-2 and PGE2, J. Cell. Physiol. 210 (3) (2007) 774–783.
[14] B.E. Crucian, S.R. Zwart, S. Mehta, P. Uchakin, H.D. Quiriarte, D. Pierson, et al., Plasma cytokine concentrations indicate that in vivo hormonal regulation of immunity is altered during long-duration spaceflight, J. Interferon Cytokine Res. 34 (10) (2014) 778–786.
[15] C. Tsatsanis, A. Androulidaki, E. Dermitzaki, I. Charalampopoulos, J. Spiess, A. Gravanis, et al., Urocortin 1 and Urocortin 2 induce macrophage apoptosis via CRFR2, FEBS Lett. 579 (20) (2005) 4259–4264.
[16] Z. Bagosi, K. Csabafi, B. Balangó, D. Pintér, O. Szolomájer-Csikós, Z. Bozsó, et al., Anxiolytic- and antidepressant-like actions of Urocortin 2 and its fragments in mice, Brain Res. 1680 (2018) 62–68.
[17] Y. Yin, J. Liu, Q. Fan, S. Zhao, X. Wu, J. Wang, et al., Long-term spaceflight composite stress induces depression and cognitive impairment in astronauts-insights from neuroplasticity, Transl. Psychiatry 13 (1) (2023) 342.
[18] M. Ouzzine, S. Gulberti, N. Ramalanjaona, J. Magdalou, S. Fournel-Gigleux, The UDP-glucuronosyltransferases of the blood-brain barrier: their role in drug metabolism and detoxication, Front. Cell. Neurosci. 8 (2014) 349.
[19] E.S. Nelson, L. Mulugeta, J.G. Myers, Microgravity-induced fluid shift and ophthalmic changes, Life 4 (4) (2014) 621–665.
[20] Y. Kutsuno, R. Hirashima, M. Sakamoto, H. Ushikubo, H. Michimae, T. Itoh, et al., Expression of UDP-glucuronosyltransferase 1 (UGT1) and glucuronidation activity toward endogenous substances in humanized UGT1 mouse brain, Drug Metab. Dispos. 43 (7) (2015) 1071–1076.
[21] A. Papadopoulos, I. Kyriakou, S. Incerti, G. Santin, P. Nieminen, I.A. Daglis, et al., Space radiation quality factor for Galactic Cosmic Rays and typical space mission scenarios using a microdosimetric approach, Radiat. Environ. Biophys. 62 (2) (2023) 221–234.
[22] S. Pätsi, A. Mishev, Ionization effect in the Earth's atmosphere due to cosmic rays during the GLE # 71 on 17 May 2012, Adv. Space Res. 69 (7) (2022) 2893–2901.
[23] Z. Li, K.K. Jella, L. Jaafar, S. Li, S. Park, M.D. Story, et al., Exposure to galactic cosmic radiation compromises DNA repair and increases the potential for oncogenic chromosomal rearrangement in bronchial epithelial cells, Sci. Rep. 8 (1) (2018) 11038.
[24] D.M. Sridharan, A. Asaithamby, S.M. Bailey, S.V. Costes, P.W. Doetsch, W.S. Dynan, et al., Understanding cancer development processes after HZE-particle exposure: roles of ROS, DNA damage repair and inflammation, Radiat. Res. 183 (1) (2015) 1–26.
[25] D.M. Sridharan, A. Asaithamby, S.R. Blattnig, S.V. Costes, P.W. Doetsch, W.S. Dynan, et al., Evaluating biomarkers to model cancer risk post cosmic ray exposure, Life Sci. Space Res. 9 (2016) 19–47.
[26] T. Oizumi, R. Ohno, S. Yamabe, T. Funayama, A.J. Nakamura, Repair kinetics of DNA double strand breaks induced by simulated space radiation, Life 10 (12) (2020).
[27] G.F. Yang, X. Zhang, Y.G. Su, R. Zhao, Y.Y. Wang, The role of the deubiquitinating enzyme DUB3/USP17 in cancer: a narrative review, Cancer Cell Int. 21 (1) (2021) 455.
[28] C. Ducker, P.E. Shaw, USP17-mediated de-ubiquitination and cancer: clients cluster around the cell cycle, Int. J. Biochem. Cell Biol. 130 (2021) 105886.
[29] C. McFarlane, A.A. Kelvin, M. de la Vega, U. Govender, C.J. Scott, J.F. Burrows, et al., The deubiquitinating enzyme USP17 is highly expressed in tumor biopsies, is cell cycle regulated, and is required for G1-S progression, Cancer Res. 70 (8) (2010) 3329–3339.
[30] S. Zhang, Z. Xu, J. Yuan, H. Chen, Ubiquitin-specific peptidase 17 promotes cisplatin resistance via PI3K/AKT activation in non-small cell lung cancer, Oncol. Lett. 20 (1) (2020) 67–74.
[31] Z. Guo, G. Zhou, W. Hu, Carcinogenesis induced by space radiation: a systematic review, Neoplasia 32 (2022) 100828.
[32] T. Akiyama, K-i Ishiguro, N. Chikazawa, S.B.H. Ko, M. Yukawa, M.S.H. Ko, ZSCAN4-binding motif—TGCACAC is conserved and enriched in CA/TG microsatellites in both mouse and human genomes, DNA Res. 31 (1) (2024) dsad029.
[33] L.-K. Tsai, M. Peng, C.-C. Chang, L. Wen, L. Liu, X. Liang, et al., ZSCAN4 interacts with PARP1 to promote DNA repair in mouse embryonic stem cells, Cell Biosci. 13 (1) (2023) 193.

[34] R. Srinivasan, N. Nady, N. Arora, L.J. Hsieh, T. Swigut, G.J. Narlikar, et al., Zscan4 binds nucleosomal microsatellite DNA and protects mouse two-cell embryos from DNA damage, Sci. Adv. 6 (12) (2020) eaaz9115.
[35] J.J. Luxton, S.M. Bailey, Twins, telomeres, and aging-in space, Plast. Reconstr. Surg. 147 (1s-2) (2021) 7s–14s.
[36] E.E. Alemasova, O.I. Lavrik, Poly(ADP-ribosyl)ation by PARP1: reaction mechanism and regulatory proteins, Nucleic Acids Res. 47 (8) (2019) 3811–3827.
[37] L.K. Tsai, M. Peng, C.C. Chang, L. Wen, L. Liu, X. Liang, et al., ZSCAN4 interacts with PARP1 to promote DNA repair in mouse embryonic stem cells, Cell Biosci. 13 (1) (2023) 193.
[38] G. Falco, S.L. Lee, I. Stanghellini, U.C. Bassey, T. Hamatani, M.S. Ko, *Zscan4*: a novel gene expressed exclusively in late 2-cell embryos and embryonic stem cells, Dev. Biol. 307 (2) (2007) 539–550.